PASJ: Publ. Astron. Soc. Japan **49**, 453–460 (1997)

Rotation Curve of the Galaxy

Mareki HONMA and Yoshiaki SOFUE
Institute of Astronomy, Faculty of Science, The University of Tokyo, 2-21-2 Osawa, Mitaka, Tokyo 181
E-mail(MH): honma@milano.mtk.nao.ac.jp

(Received 1996 October 25; accepted 1997 April 10)

Abstract

Reanalyzing the galactic H I survey data with two methods which make use of the geometry of the galactic disk, we explore the outer rotation curve. In addition to the derivation of the outer rotation curve, we investigate their uncertainties, which have not been established previously. Comparing with those obtained previously based on various methods, we find that the rotation curve obtained by the method of Merrifield has the smallest error and the largest coverage of galacto-centric radius among the existing rotation curves. Combining with the inner rotation curve obtained previously by the H I tangential velocity, we present the overall rotation curve of the Galaxy, which ranges from $0.3R_0$ to $2.5R_0$. The rotation curve is gradually rising with the galacto-centric radius if the IAU standard galactic constants, $R_0 = 8.5$ kpc and $\Theta_0 = 220$ km s^{-1}, are assumed. However, the shape of the rotation curve is fairly sensitive to the adopted values of the galactic constants, and the outer rotation curve could be declining if Θ_0 is smaller than 200 km s^{-1} .

Key words: Dark matter — Galaxies: Milky Way — Rotation

1. Introduction

The rotation curve is one of the most powerful tools for studying the dynamics of galaxies. Rotation curves have been derived for many external galaxies based on optical and radio observations (e.g., Bosma 1981; Rubin et al. 1985; Sofue 1996). The rotation curves of spiral galaxies are usually flat, even beyond the optical disk, indicating the existence of dark matter.

As for the Milky Way Galaxy, the inner and outer rotation curves have been derived by different methods. Under an assumption of axisymmetry, the radial velocity of an object in a circular orbit is given by

$$V_r = W(R)\sin l, \tag{1}$$

where

$$W(R) = \left[\Theta(R)\left(\frac{R_0}{R}\right) - \Theta_0\right]. \tag{2}$$

Here, R and Θ are the radius and the rotation velocity at a point of the Galaxy; subscript 0 denotes the value at the Sun. In the inner Galaxy the radial velocity along a line of sight becomes maximum at the closest point to the galactic center, i.e., the tangential point. Since the distance from the galactic center to a tangential point is uniquely given by $R = R_0 \sin l$, the inner rotation curve has been derived by the tangential velocity of H I and CO emission (e.g., Burton, Gordon 1978; Clemens 1985; Fich et al. 1989). In figure 1 we show the inner rotation curves of the Galaxy obtained from the H I tangential velocity (Fich et al. 1989) and the CO tangential velocity (Clemens 1985), as well as that obtained from planetary nebulae (Schneider, Terzian 1983). The rotation curve in the central region ($R \leq 0.3R_0$) is taken from Burton and Gordon (1978), and the IAU standard Θ_0 of 220 km s^{-1} is assumed. While the rotation curve obtained from planetary nebulae lies slightly below those obtained by H I or CO, the H I and CO rotation curves (CO is only for the northern hemisphere) agree with each other, except for local deviations.

In the outer Galaxy, however, such a method cannot be applied because there is no tangential point along a line of sight. Instead, the outer rotation curve was obtained by measuring the distances and radial velocities of many galactic objects, such as H II regions, planetary nebulae, and stars (e.g., Blitz 1979; Schneider, Terzian 1983; Clemens 1985; Fich et al. 1989; Brand, Blitz 1993; Turbide, Moffat 1993; Amaral et al. 1996; Pont et al. 1997). In figure 1 we show the outer rotation curve obtained by H II regions (Brand, Blitz 1993) and by planetary nebulae (Schneider, Terzian 1983). In both cases the uncertainty in the outer rotation curve is fairly large when compared with the inner rotation curve. This may be partly due to an error in the estimate of the distance, and partly due to the limited sample of galactic objects. Moreover, there could be some systematic errors in determining the distance to the objects, since the metallicity gradient in the outer Galaxy is not determined well (see

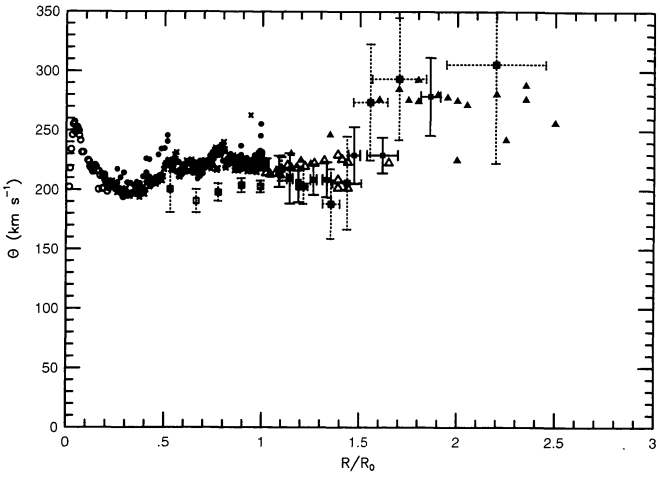

Fig. 1. Rotation curves of the Galaxy so far obtained. The open circles are the H I tangential velocity from Burton and Gordon (1978), the filled circles are H I from Fich et al. (1989), and the crosses are CO from Clemens (1985). The open squares are of Planetary Nebulae (Schneider, Terzian 1983), the filled square are of H II regions (Brand, Blitz 1993). The triangles are the rotation velocities obtained using the geometry of the Galaxy's disk; the filled triangles by Merrifield (1992), and the open triangles by Petrovskaya and Teerikorpi (1986).

Brand, Blitz 1993).

Alternatively, two methods, which make use of the geometry of the H I disk and do not require any measurements of galactic objects, have been developed (Petrovskaya, Teerikorpi 1986; Merrifield 1992). Given a fixed value of $W(R)$ in equation (1), one can extract an H I ring centered on the galactic center from the H I disk. If the ring radius R is known, one can obtain the rotation velocity at R from equation (2). Merrifield (1992) has introduced the assumption of a constant thickness along each H I ring, and obtained the ring radii R. Under that assumption, the angular thickness Δb of an H I ring is given by

$$\Delta b = \arctan\left(\frac{z_0}{R_0\cos l + \sqrt{R^2 - R_0^2\sin^2 l}}\right), \qquad (3)$$

where l and z_0 denote the galactic latitude and the constant thickness. Applying this to the observed angular thickness of the H I rings, one can determine R and z_0. On the other hand, Petrovskaya and Teerikorpi (1986) have used the H I brightness temperature to obtain the ring radii under the assumption that the H I gas density is constant along a ring. With this assumption the brightness temperature T_b is given by

$$T_\mathrm{b} = \frac{1}{X_{\mathrm{H\,I}}} n(R) \left|\frac{d\Theta}{dR} - \frac{\Theta}{R}\right|^{-1} \times \left[\frac{R_0}{R}|\sin l|\sqrt{1 - R_0^2 R^{-2}\sin^2 l}\right]^{-1}, \qquad (4)$$

where $X_{\mathrm{H\,I}}$ is the conversion factor and $n(R)$ is the gas density.

We show in figure 1 the results obtained by Merrifield (1992) and by Petrovskaya and Teerikorpi (1986). These rotation curves agree with those obtained from the H II regions or planetary nebulae, and have as large an extent as others. Moreover, these methods have the following advantages; 1) these methods make use of the H I data of the entire galactic disk, so that the local effect is expected to be small, and 2) the distance measurement is rather direct. However, the uncertainty in the rotation curves obtained by these methods has not yet been well studied well. Since the outer rotation curve provides bases for studies of the outer Galaxy and the dark halo, the uncertainty in these rotation curves should be established. In this paper we reanalyze the galactic H I survey data by applying the two methods described above in order to derive the outer rotation curves and their uncertainties. With these rotation curves and uncertainties, we investigate which rotation curve is most reliable at present.

2. Derivation of Outer Rotation Curve

2.1. Data

We reanalyzed the galactic H I survey data on the basis of the two methods described in section 1. The data which we used were taken from Weaver and Williams (1974) for the northern hemisphere and from Kerr et al. (1986) for the southern hemisphere. The set of data covers the region $l = 10°$ to $350°$ and $|b| \leq 10°$. The coverage of the galactic latitude is wide enough to see the entire distribution of H I gas in the b direction, except for the local region of the Sun. All of the data are in the form of a latitude-velocity diagram, sampled every $0.°5$ in longitude and every $0.°25$ in latitude. The velocity resolution is 2.1 km s^{-1} for both data. The angular resolution is $35.'5$ for the data of Weaver and Williams and $48'$ for the data of Kerr et al. The brightness temperature of the data was scaled so that the brightness temperatures from both data are equal in the overlapped region ($l = 240°$ to $250°$). The brightness temperature in the outer region is typically more than 5 K, whereas the rms noise is around 0.3 K. Therefore, the observational uncertainty is sufficiently small in the present analysis.

2.2. Analysis

For the method by Merrifield (1992), the angular thickness of the H I disk was calculated from the H I density distribution in the b direction. Considering that the H I density is proportional to the brightness temperature T_b when the optical depth is small, we defined the angular thickness Δb by

$$\Delta b^2 = \frac{\Sigma (b_i - b_0)^2 \times T_i^4}{\Sigma T_i^4}, \tag{5}$$

where T_i is the brightness temperature at galactic latitude b_i, and b_0 is the centroid of the gas distribution defined by

$$b_0 = \frac{\Sigma b_i \times T_i^4}{\Sigma T_i^4}, \tag{6}$$

which satisfies $\partial \Delta b / \partial b_0 = 0$. The brightness temperature is weighted by T_i^4 instead of T_i^2 so that the thus-calculated angular thickness is not affected by the diffuse extended H I gas (e.g., Lockman 1984; Dickey, Lockman 1990). We note that if the H I density distribution in the b direction is Gaussian one, Δb defined by equation (3) gives the scale length of the Gaussian function, equal to a $1/e$ Gaussian scale length multiplied by a factor of $1/(2\sqrt{2}) \approx 0.35$.

For the method by Petrovskaya and Teerikorpi (1986), the brightness temperature T_b for a small optical depth is given by equation (4). For convenience in the least-squares fitting, we used the following equations proposed by Petrovskaya and Teerikorp instead of equation (4):

$$1/\left(T_\mathrm{b}^2 \sin^2 l\right) = C(R)^2 \left(1 - \frac{R_0^2 \sin^2 l}{R^2}\right), \tag{7}$$

where

$$C(R) = \frac{X_{\mathrm{H\,I}}}{n(R)} \left[\frac{d\Theta}{dR} - \frac{\Theta}{R}\right] \frac{R_0}{R}. \tag{8}$$

The brightness temperature is averaged in the b direction, where the temperature is larger than half of the peak temperature.

In both methods, the ring radius R is always coupled with R_0 as R/R_0 [see equations (2), (3), (4), and (7)]. Therefore, the relative ring radius R/R_0, rather than the absolute ring radius R, is obtained in the following analyses.

2.3. *Effect of Warp*

Here, we examine the effect of the warp in the outer disk. Figure 2 shows the variation of the centroid b_0 for three rings: $W(R) = -30$ km s^{-1}, -70 km s^{-1}, and -100 km s^{-1} (the radii of these rings will be found to be $1.14R_0$, $1.68R_0$, and $2.22R_0$ in the following subsection). Figure 2 clearly demonstrates the variation of the centroids with the galactic longitude l, i.e., the warp of the outer H I disk. However, the variations of the centroid are well fitted by a sine curve for all cases. Such a variation occurs when the gas motion is circular and the orbital plane is rotated with respect to the galactic plane around the line of sight to the galactic center. Hence, one can expect that the gas motion in the warped H I disk is nearly circular, and thus the methods described above can be applied. In the warped region, the thickness Δb

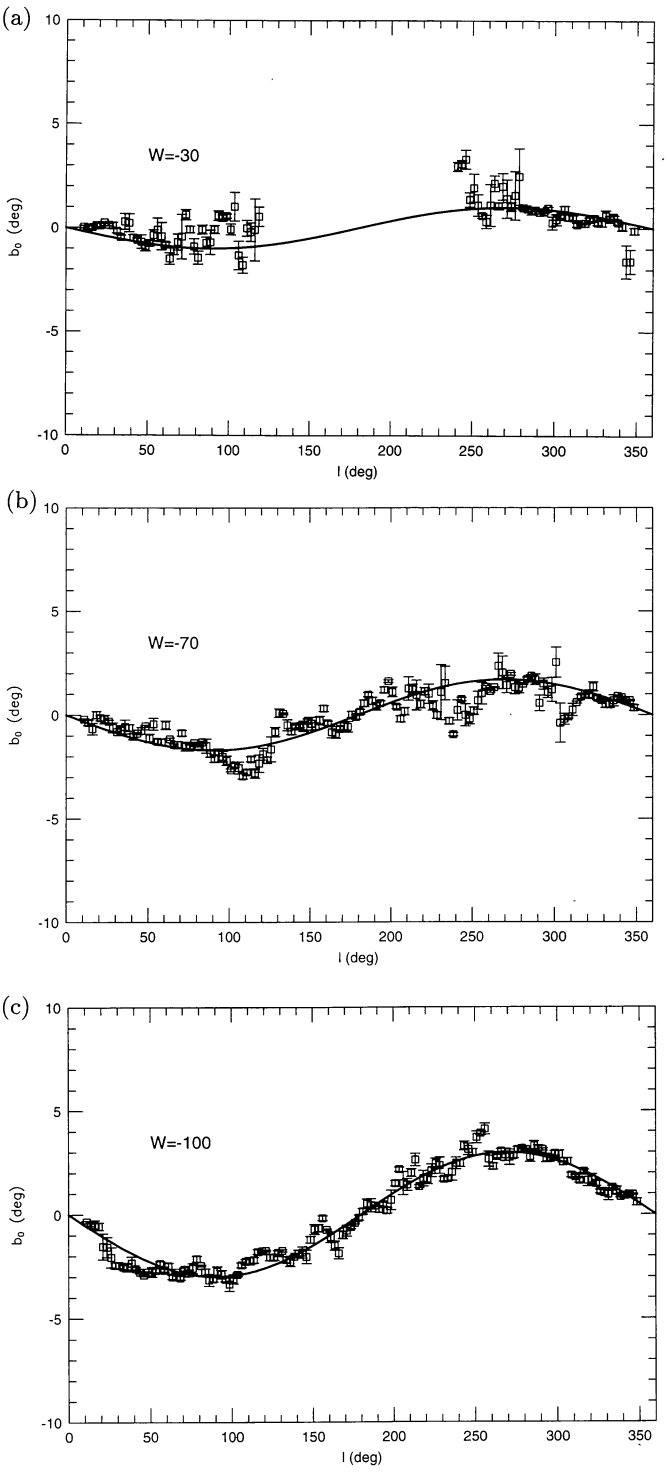

Fig. 2. Variations of the observed centroid of a gas layer with galactic longitude l. The three cases correspond to $W(R)$ of -30 km s^{-1}, -70 km s^{-1}, and -100 km s^{-1}. The fitted sine curves are superposed on them. The data between $l = 120°$ and $240°$ are excluded for $W(R) = -30$ km s^{-1}, since the gas distributes beyond the observed range of galactic latitude b.

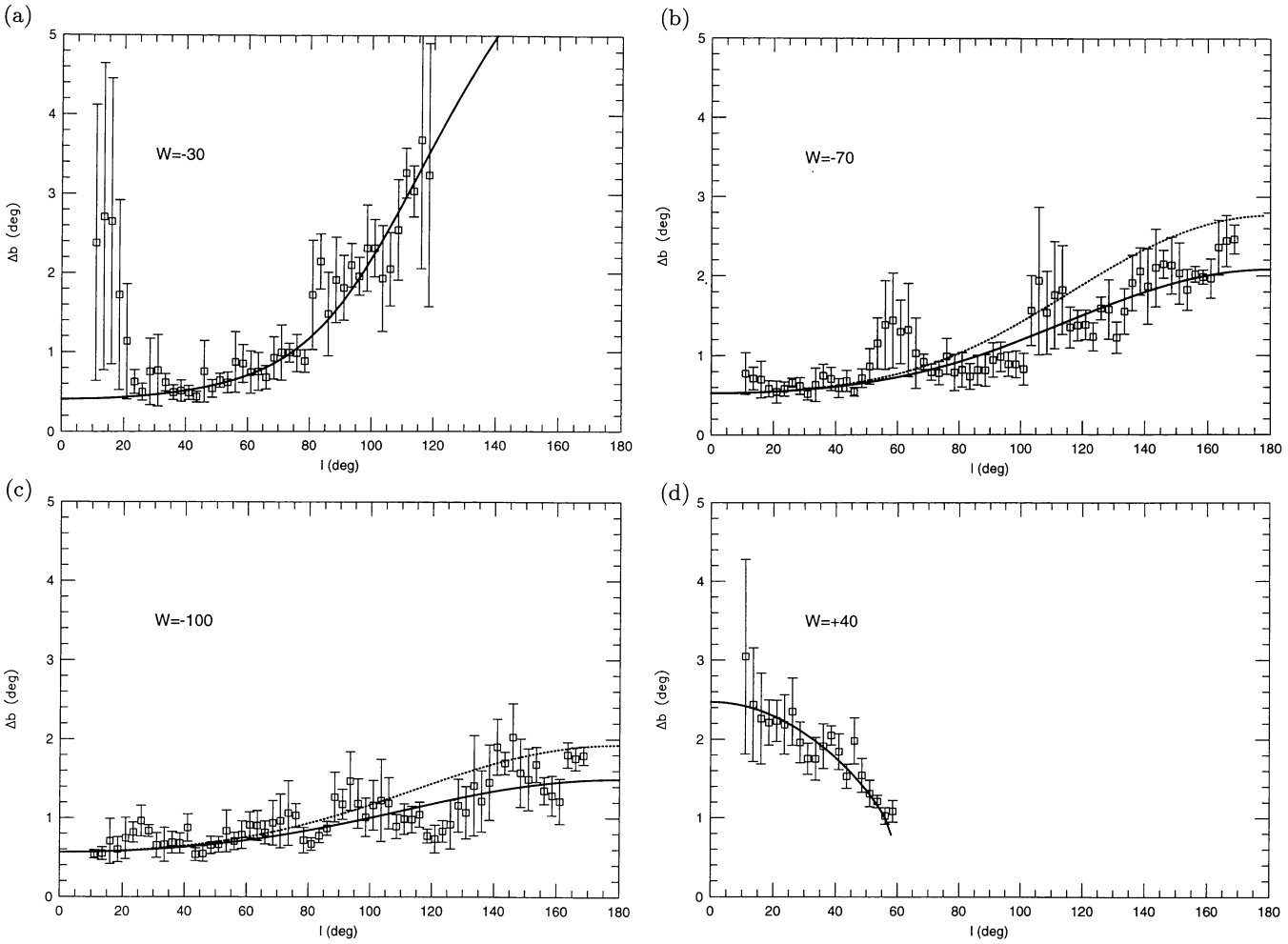

Fig. 3. Angular thickness Δb with galactic longitude l. The thick lines are the best-fit lines to the data [equation (3)]. For $W(R) = -30$ km s^{-1} the data for $l \geq 120°$ are excluded because the H I gas distributes beyond the observed range of b. The dotted lines in figures 3b and 3c are the variation in the angular thickness predicted by a flat rotation curve. For dotted lines z_0 is chosen so that the angular thickness at $l = 0°$ is equal to the best-fit line. Figure 3d shows the variation in the angular thickness for an inner ring [$W(R) = +40$ km s^{-1}].

of a ring is measured perpendicularly from the tilted ring plane.

2.4. Fitting and Uncertainty Estimate

On the basis of equations (1) and (2), we extracted the H I rings from the H I data cube. We averaged the data between two rings which correspond to $W(R) - \delta W$ and $W(R) + \delta W$, respectively. The value of δW was taken to be 5.8 km s^{-1}, so that $2 \times \delta W \sin l$ at $l = 10°$ and 170° are 2 km s^{-1}, which corresponds to the velocity resolution of the data. The data within 10° of the direction of the galactic center and the anti-center were excluded from our analysis because of the degeneracy of the radial velocity. Both Δb and T_b were averaged between the northern part and the southern part of the disk, and averaged every 2°.5 longitude interval.

Figures 3 show the angular thickness Δb for four cases of $W(R)$ as a function of l. We performed least-squares fittings for Δb according to equation (3). The results are shown by the thick lines in figure 3. The dotted lines in figures 3b and 3c show the variations of Δb when a flat rotation curve of $\Theta_0 = 220$ km s^{-1} is assumed. The difference between the observed thickness variation and that derived from the flat rotation curve is substantial; the best-fit lines lie below those obtained by the flat rotation curve. This indicates that the ring radii R are larger than that derived from the flat rotation curve. Figure 3d shows the angular thickness for a ring in the inner Galaxy. The variation in the thickness yields the radius and rotation velocity of this ring to be $0.85R_0$ and 221 km s^{-1} if $\Theta_0 = 220$ km s^{-1}. The result is in good agreement with the inner rotation curve determined by the tangential methods (e.g., Burton, Gordon 1978; Fich et al. 1989).

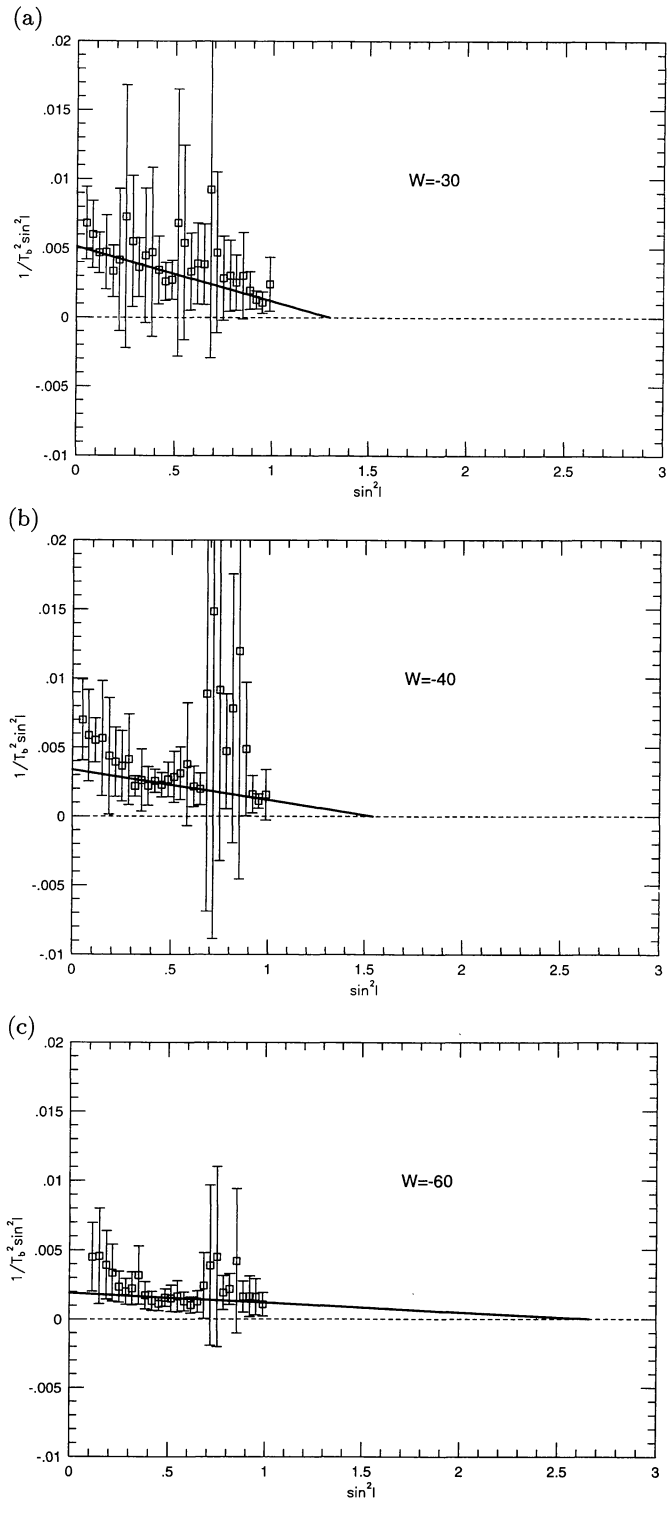

Fig. 4. Variation of $(1/T_b^2 \sin^2 l)$ against $\sin^2 l$ (see equation 7). The best-fit lines are shown by the thick lines. The intercept of the best-fit line with the dashed line corresponds to $(R/R_0)^2$.

Table 1. Results of a least-squares fitting.

	Method 1			Method 2	
$W(R)$(km s^{-1})	R/R_0	σ_r	z_0/R_0	R/R_0	σ_r
−30.....	1.14	0.037	0.13	1.14	0.19
−35.....	1.30	0.088	0.17	...	...
−40.....	1.41	0.100	0.17	1.24	0.28
−50.....	1.49	0.121	0.16	...	...
−60.....	1.59	0.110	0.18	1.63	0.46
−70.....	1.68	0.101	0.21	...	...
−75.....	1.80	0.118	0.24	...	...
−80.....	1.96	0.173	0.28	...	...
−90.....	2.11	0.155	0.30	...	...
−100.....	2.22	0.276	0.27	...	...
−110.....	2.44	0.277	0.31	...	...
−120.....	2.53	0.345	0.34	...	...
+40	0.85	0.026	0.06	...	...

Notes. Methods 1 and 2 correspond to that by Merrifield (1992) and by Petrovskaya and Teerikorpi (1986), respectively. The value of $W(R)$ was taken to be −30, −40, ... in km s^{-1}. We added results for −35 and −75 km s^{-1}, where R changes drastically with $W(R)$. σ_r is the standard deviation of the data from the best-fit line. For method 2, we obtain results for only $W(R) = -30$, −40, and −60 km s^{-1}. For other values of $W(R)$, since σ_r is found to be larger than 0.5, the deviation is too large to derive a reliable rotation curve.

Similarly, the fitting to equation (7) was performed using the methods of Petrovskaya and Teerikorpi (1986). Figure 4 shows $1/(T_b^2 \sin^2 l)$ against $\sin^2 l$ and the best-fit lines. The intercept of the best-fit lines with dashed lines gives $(R/R_0)^2$. We calculated the ring radius R/R_0 for $W(R) = -30$, −40,..., −120 km s^{-1}, and for $W(R) = -35$ and −75 km s^{-1} where R/R_0 changes rapidly with $W(R)$. Then, the rotation velocity $\Theta(R)$ of each ring is obtained by equation (2). The uncertainty σ_r of the ring radii were also estimated for each ring. The uncertainty σ_r is defined as the 1-σ deviation of the observed angular thickness or brightness temperature from the best-fit curve (equation 3 or 7). The uncertainty in the ring radii causes an uncertainty in the rotation velocity through equation (2). Such an uncertainty in the rotation velocity is given by $\sigma_r \times [W(R) + \Theta_0]$. The results for R/R_0 and σ_r are listed in table 1 for both methods. The rotation velocities of the rings obtained by both methods are shown in figure 5. The rotation velocities previously obtained by Merrifield (1992) and Petrovskaya and Teerikorpi (1986) are also plotted. The two rotation curves derived in the present study are consistent with each other within the errors. The present and Merrifield's results are also in good agreement, except around $R \sim 1.7R_0$. The difference might come

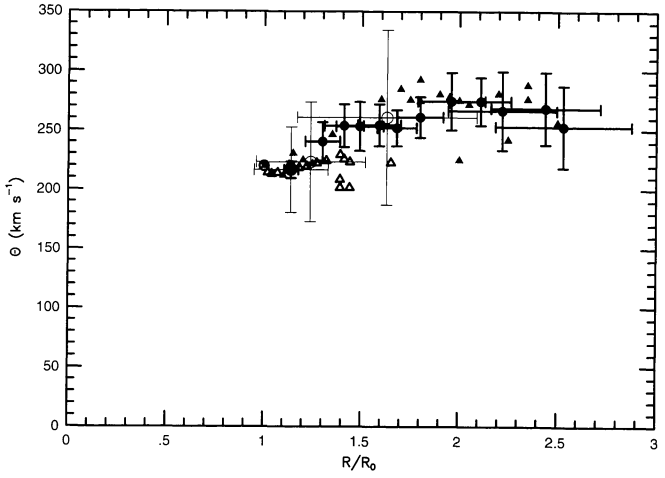

Fig. 5. Rotation curves obtained in the present paper. The filled and open circles are those obtained by Merrifield's method and by the method of Petrovskaya and Teerikorpi, respectively. Filled triangles are the results taken from Merrifield (1992), and open triangles are the results taken from Petrovskaya and Teerikorpi (1986). R_0 and Θ_0 are assumed to be 8.5 kpc and 220 km s^{-1}, respectively.

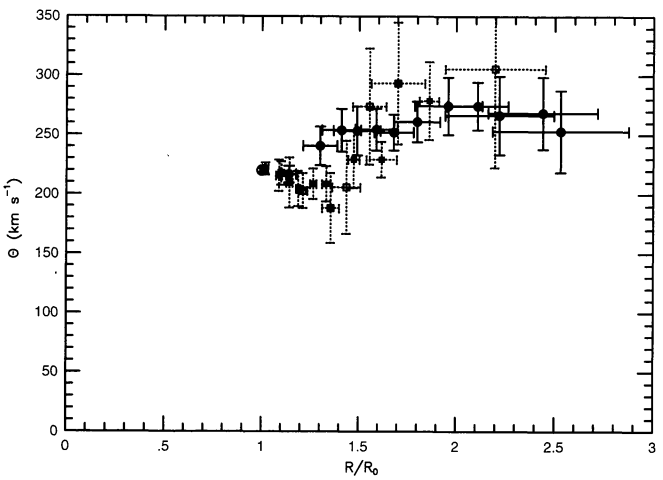

Fig. 6. Outer rotation curve obtained by Merrifield's method (filled circles) superposed on those obtained by other methods. The filled square are the rotation velocity obtained from H II regions (Brand, Blitz 1993). The open squares are the rotation velocity obtained from planetary nebulae (Schneider, Terzian 1983). R_0 and Θ_0 are assumed to be 8.5 kpc and 220 km s^{-1}, respectively.

from the effect of the velocity dispersion of H I gas; while $2 \times \delta W(R)$ in Merrifield (1992) equals 5 km s^{-1}, we take 11.6 km s^{-1}, which is set to be comparable to the velocity dispersion of H I gas in the Galaxy and external galaxies (e.g., Dickey, Lockman 1990; van der Kruit, Shostak 1983, 1984), $\sim$ 10 km s^{-1}. Figure 5 also demonstrates that the rotation curve obtained by Merrifield's method has smaller uncertainties than the other. The typical uncertainty of the rotation velocities obtained by Merrifield's method is found to be less than 30 km s^{-1}. Therefore, the rotation curve by Merrifield's method is better both in the accuracy of the rotation velocity and in the radial extent.

3. Overall Rotation Curve of the Galaxy

Here, we compare the rotation curve obtained above by Merrifield's method with those obtained by various methods. Figure 6 illustrates the rotation velocities derived from the H II regions by Brand and Blitz(1993), those from planetary nebulae by Schneider and Terzian (1983), and the present ones obtained by Merrifield's method. All of the rotation velocities are in agreement in the sense that they show the tendency of increasing with the galacto-centric distance. However, the uncertainties of the rotation velocities derived from the H II regions and planetary nebulae are larger than those obtained by Merrifield's method. The uncertainty in the rotation velocities by Merrifield's method is estimated to be 30 km s^{-1} at the maximum, which is less than half of that for planetary nebulae at $R_0 \geq 2.0$. Since the outer rotation velocities derived by Merrifield's method has the smallest error and the largest coverage of the galacto-centric radius among the existing outer rotation curve, the rotation curve derived by Merrifield's method is the most reliable one at present.

Combining the outer rotation curve with the inner one previously established, we obtain the overall rotation curve of the Galaxy. The inner rotation curve is derived from the H I tangential velocity; the data are taken from Fich et al. (1989) and averaged every $0.1R_0$ (table 2). Thus, the obtained rotation curve ranges from $0.3R_0$ to $2.5R_0$.

In order to obtain a definite rotation curve of the Galaxy, however, accurate galactic constants are required, because the rotation velocity $\Theta(R)$ derived by equation (2) depends on the adopted values of Θ_0. While the IAU standard value of Θ_0 is 220 km s^{-1}, several studies claim smaller values of Θ_0 (e.g., Rohlfs et al. 1986; Merrifield 1992; Kuijken, Tremaine 1994). Moreover, recent studies of the distance to the galactic center R_0 claim a smaller value than the IAU value of 8.5 kpc (e.g., Reid et al. 1988; Reid 1993). The smaller value of R_0 gives a smaller Θ_0 again through the relation,

$$\frac{\Theta_0}{R_0} = A - B, \tag{9}$$

where A and B are the Oort constants, and are determined fairly well (e.g., Kerr, Lynden-Bell 1986;

Table 2. Data for the inner rotation curve from the H I tangent points.

R/R_0	$W(R)$(km s^{-1})	σ_W(km s^{-1})
0.35.....	361.5	45.1
0.45.....	262.8	35.9
0.55.....	190.9	36.9
0.65.....	116.3	18.5
0.75.....	82.7	8.2
0.85.....	45.4	9.2
0.95.....	13.4	8.1

Note. Data were taken from Fich et al. (1989). σ_W is 1-σ deviation of $W(R)$.

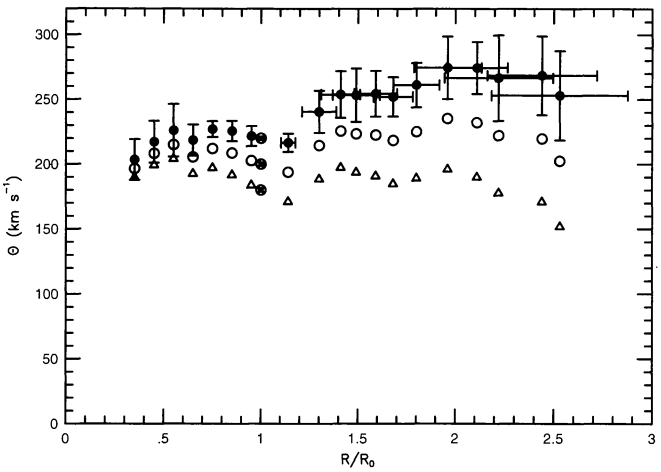

Fig. 7. Overall rotation curves of the Galaxy for $\Theta_0 =$ 220 km s^{-1} (filled circles), $\Theta_0 = 200$ km s^{-1} (open circles), and $\Theta_0 = 180$ km s^{-1} (open triangles). The data for the inner rotation curve were taken from Fich et al. (1989). The outer rotation curve are those obtained by Merrifield's method. The error bars are indicated only for $\Theta_0 = 220$ km s^{-1}, and are almost the same for the three cases.

Miyamoto et al. 1993). To see how Θ_0 affects on the shape of the rotation curves, we give the rotation curves obtained by assuming $\Theta_0 = 220$ km s^{-1}, 200 km s^{-1}, and 180 km s^{-1} in figure 7. Figure 7 clearly demonstrates that the shape of the outer rotation curve is sensitive to the value of Θ_0. In the case $\Theta_0 = 220$ km s^{-1}, the outer rotation curve is rising from $1.1R_0$ to $2R_0$ by more than 50 km s^{-1}, as has been stated previously (e.g., Brand, Blitz 1993). Although the rotation curve for $\Theta = 200$ km s^{-1} is rising slightly, it is not as steep as that for $\Theta_0 = 220$ km s^{-1}, and the rotation curve for $\Theta_0 = 180$ km s^{-1} is almost flat, or slightly falling. These results imply that the mass distribution in the Galaxy derived from the rotation curve is also sensitive to the adopted value of Θ_0 (see Honma, Sofue 1996).

Although the rotation curve within $2R_0$ is rising or flat, depending on Θ_0, the rotation curves beyond $2R_0$ show a tendency to decline for all cases. This may be related to the cutoff of the optical disk, which occurs at about $2R_0$ (Robin et al. 1992; Ruphy et al. 1996), since this kind of correlation is also seen in other galaxies (e.g., NGC 4013, Bottema et al. 1987; NGC 4244, Olling 1996).

4. Discussion

On the basis of the thus-obtained rotation curve thus obtained, we can derive the total galactic mass enclosed within radius R from the relation $M(R) = R\Theta(R)^2/G$ under the assumption of a spherical mass distribution. The results are described elsewhere (Honma, Sofue 1996), from which we report that the total galactic mass could be much smaller than that estimated from a flat rotation curve.

Since the mass distribution in the outer Galaxy inferred from the rotation curve depends strongly on the galactic constants, R_0 and Θ_0, an accurate determination of the constants is essential. If the shape of the rotation curve is universal, as suggested by Persic et al. (1996), one may use the shape of the rotation curve to constrain the galactic constants. As can be seen in figure 7 the outer rotation curve rises by more than 50 km s^{-1} in the case of $\Theta_0 = 220$ km s^{-1}. This is not likely in other spiral galaxies with a similar luminosity; spiral galaxies as luminous as the Galaxies are likely to have a flat rotation curve (e.g., Bosma 1981; Rubin et al. 1985; Persic et al. 1996). If we assume that the rotation curve of the Galaxy is also flat, Θ_0 should be reduced to less than 200 km s^{-1}. Based on a similar analysis Merrifield (1992) has suggested that Θ_0 is 200 ± 10 km s^{-1}.

On the other hand, one can obtain Θ_0 through equation (9) once R_0 is measured. R_0 can be obtained by a comparison of the kinematic distance of galactic objects calculated from a rotation curve with the real distance of the objects. Honma and Sofue (1996) used the rotation curve obtained in this paper and the data of OH/IR stars and of young stars in the outer disk, and obtained an R_0 of 7.6 kpc, which is in good agreement with recent studies of R_0 (e.g., Reid et al. 1988; Reid 1993). With the Oort's galactic constants, $A - B = 25.8 \pm 0.8$ km s^{-1} kpc^{-1}, obtained by Miyamoto et al. (1993), an R_0 of 7.6 kpc yields a Θ_0 of 196 km s^{-1}. These results indicate that a Θ_0 of about 200 km s^{-1} and an R_0 less than 8 kpc are more favorable than the IAU standard values.

We thank the referee, Masanori Miyamoto, for helpful suggestions in improving the manuscript. M.H. was financially supported by the Japan Society for the Promotion of Science.

References

Amaral L.H., Ortiz R., Lépine J.R.D., Maciel W.J. 1996, MNRAS 281, 339
Blitz L. 1979, ApJ 231, L115
Bosma A. 1981, AJ 86, 1825
Bottema R., Shostak G.S., van der Kruit P.C. 1987, Nature 328, 401
Brand J., Blitz L. 1993, A&A 275, 67
Burton W.B., Gordon M.A. 1978, A&A 63, 7
Clemens D.P. 1985, ApJ 295, 422
Dickey J.M., Lockman F.J. 1990, ARA&A 28, 215
Fich M., Blitz L., Stark A.A. 1989, ApJ 342, 272
Honma M., Sofue Y. 1996, PASJ 48, L103
Kerr F.J., Bowers P.F., Jackson P.D., Kerr M. 1986, A&AS 66, 373
Kerr F.J., Lynden-Bell D. 1986, MNRAS 221, 1023
Kuijken K., Tremaine S. 1994, ApJ 421, 178
Lockman F.J. 1984, ApJ 283, 90
Merrifield M.R. 1992, AJ 103, 1552
Miyamoto M., Soma M., Yoshizawa M. 1993, AJ 105, 2138
Olling R.P. 1996, AJ 112, 457
Persic M., Salucci P., Stel F. 1996, MNRAS 281, 27
Petrovskaya I.V., Teerikorpi P. 1986, A&A 163, 39
Pont F., Queloz D., Bratschi P., Mayor M. 1997, A&A 318, 416
Reid M.J. 1993, ARA&A 31, 345
Reid M.J., Schneps M.H., Moran J.M., Gwinn C.R., Genzel R., Downes D., Rönnäng B. 1988, ApJ 330, 809
Robin A.C., Crézé M., Mohan V. 1992, ApJ 400, L25
Rohlfs K., Chini R., Wink J.E., Böhme R. 1986, A&A 158, 181
Rubin V.C., Burstein D., Ford W.K. Jr, Thonnard N. 1985, ApJ 289, 81
Ruphy S., Robin A.C., Epchtein N., Copet E., Bertin E., Fouqué P., Guglielmo F. 1996, A&A 313, L21
Schneider S.E., Terzian Y. 1983, ApJ 274, L61
Sofue Y. 1996, ApJ 458, 120
Turbide L., Moffat F.J. 1993, AJ 105, 1831
van der Kruit P.C., Shostak G.S. 1983, A&A 105, 351
van der Kruit P.C., Shostak G.S. 1984, A&A 134, 258
Weaver H., Williams D.R.W. 1974, A&AS 17, 1